

Optimization of FTS Phase Correction Parameters

L. D. Spencer and D. A. Naylor

*Department of Physics, University of Lethbridge, 4401 University Drive, Lethbridge, Alberta, T1K 3M4, Canada
Locke.Spencer@uleth.ca*

Abstract: Phase correction is critical for extracting accurate spectral information from the Fourier transform of interferograms. We discuss common sources of phase errors and the optimization of phase correction parameters required for their rectification.

©2005 Optical Society of America

OCIS codes: (070.2590) Fourier Transforms; (300.6300) Spectroscopy, Fourier Transforms

1. Introduction

It is often desirable to operate an FTS in the single-sided mode to maximize the attainable resolution for a given length of translation stage. However, single-sided interferograms contain only low resolution phase information, which, if left uncorrected, will introduce artefacts into the final spectrum, limiting the accuracy of derived spectral parameters. There are several causes of phase errors in FTS instruments, including offsets due to electronic amplifiers, optical path sampling errors, beam splitter dispersion, and distortion arising from variations in the speed of the translation stage introduced through the detector time constant or data acquisition electronics. Phase correction is a technique used to correct for the asymmetry in a single-sided interferogram.

2. Phase Correction

Spectral phase is determined by computing the arc tangent of the ratio of the imaginary and real parts of a spectrum. The spectrum from an ideal FTS should have no imaginary component and thus have zero phase. Various aspects of any real interferometer introduce imaginary components into the spectrum: Optics and electronics may introduce systematic phase errors which can often be well characterized. Random noise contributes equally to the real and imaginary domains. Proper phase correction should leave half of the random noise behind in the imaginary component of the spectrum, which is ignored after phase correction.

An ideal interferogram will contain exactly the same information on one side of the zero path difference (ZPD) position as on the other, and so in theory only one side of the interferogram needs to be measured. In practice, the above mentioned issues make it necessary to measure at least a short double-sided interferogram to characterize the instrumental phase and single-sided interferograms are measured with a low resolution double-sided component. Once the phase of the instrument has been determined from a short double-sided region of the interferogram, it can be used to restore the symmetry of the high-resolution, single-sided part of the scan. Given a translation stage of fixed length, this leads to a trade-off between the travel used to determine phase information and that used to achieve a higher spectral resolution.

3. Phase Correction and Parameter Optimization Investigation Software

Software was developed to investigate the parameter dependencies involved in phase correction. Input spectra consist of Gaussian absorption lines superimposed on a continuum. The spectra are Fourier transformed to produce interferograms, which are then subject to a phase error. The phase correction software allows the following parameters to be varied: double-sided length of the interferogram, double-sided apodization type, phase correction function (PCF) length, and PCF apodization type. The asymmetric interferograms are phase corrected using different processing parameters and the retrieved spectra are then compared to the original.

3.1. Input Spectra

Four input spectra were generated from a Gaussian background continuum with 5 superimposed Gaussian absorption lines of varying widths. The continuum is identical in each spectrum; the absorption lines (of depth 50% of the continuum) have widths (FWHM) of 1, 5, 10, and 25 times the spectral resolution. ZPD sampling phase errors are generated by shifting the ideal interferogram sampling by 0 to 3 points. The input data is shown in Figure 1.

3.2. Phase Correction Procedure

The ideal interferogram, $I(x)$, is given by the Eq. 1, where $B(\sigma)$ is the source spectrum and x is the interferogram optical path difference (OPD).

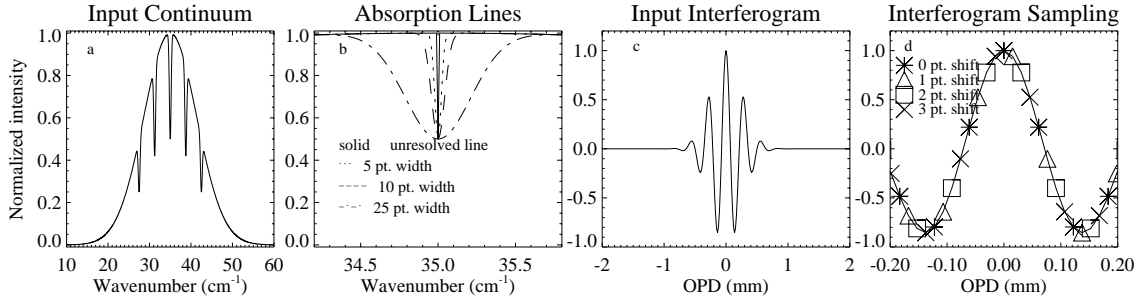


Fig. 1. Gaussian continuum (a) with absorption lines (b) and corresponding interferogram (c) with sampling shown near ZPD (d).

$$I(x) = \int_0^\infty B(\sigma) \cos(2\pi\sigma x) d\sigma \quad (1)$$

A real interferogram will contain additional components:

$$I(x) = \int_0^\infty [B(\sigma) * 2L \text{sinc}(2L\sigma)] e^{i(\phi)} \cos\left[2\pi\sigma x \left(1 - \frac{\Omega_M}{4\pi}\right)\right] d\sigma \quad (2)$$

where the phase, ϕ , has several components:

$$\phi = \phi_{DC} + \phi_{ZPD}\sigma + \phi_{NL}(\sigma) + \phi_R(\sigma) \quad (3)$$

In these equations, L is the maximum OPD of the interferogram, ϕ_{DC} is a fixed phase offset, ϕ_{ZPD} is a linear phase due to ZPD sampling error, $\phi_{NL}(\sigma)$ is a non-linear phase component (due to a beamsplitter for example), and $\phi_R(\sigma)$ a random phase element due to noise. The sinc convolution in Eq. 2 is due to the finite maximum OPD of the FTS and the last term accounts for natural apodization resulting from divergence of the beams within the interferometer. In principle, ϕ_{DC} and ϕ_{NL} are stable and can be either measured or calculated. The linear phase error, ϕ_{ZPD} , can then be determined from a measurement of the phase obtained from a short double-sided interferogram. We use the Forman et al phase correction method [2] in which the phase correction function, defined as:

$$PCF = FT^{-1}(e^{-i\phi}) \quad (4)$$

is convolved with the original asymmetric interferogram to produce a symmetric one, effectively redistributing energy within the interferogram. As with any convolution in the spatial domain, the potential exists for introducing spectral artefacts. These, however, can be minimized by the use of apodizing functions at different stages in the analysis (apodizing the double-sided interferogram prior to phase determination, the PCF, and/or the single-sided interferogram). While apodization of the interferograms before Fourier transformation reduces the amplitude of the sidelobes of spectral features, apodization of the PCF reduces the range over which interferogram energy may be redistributed during convolution but with potential reduction of the effectiveness of the phase correction procedure. The convolution of the original interferogram with the PCF also reduces the overall spectral resolution, since convolution truncates the interferogram by one half the length of the PCF.

The phase correction software was written in IDL[®] [3] and follows a modular design. The double-sided portion of the interferogram is extracted and used to generate a low resolution spectrum. The spectral phase is determined and used to generate the phase error, ϕ . Finally, the PCF is determined (Eq. 4) and convolved with the original interferogram to produce the symmetric interferogram. Fig. 2 shows various stages in the phase correction process. The final phase corrected interferogram is then Fourier transformed resulting in the high resolution spectrum.

3.3. Procedure

The same set of input spectra were processed to generate an 8-dimensional set of processing error data. The dimensions are: phase error, double-sided width, PCF width, double-sided apodization, PCF apodization, line width, line centre, and error type. Double-sided interferogram and phase correction widths were modified from 8 points to 512 (the maximum available in our case). Ten different apodization schemes were applied to the interferogram and the phase correction function, producing line broadening ranging from 1 to 2 times the unapodized FWHM. Every possible parameter combination and the associated spectral errors (~25 million combinations) were entered into the multidimensional set for analysis.

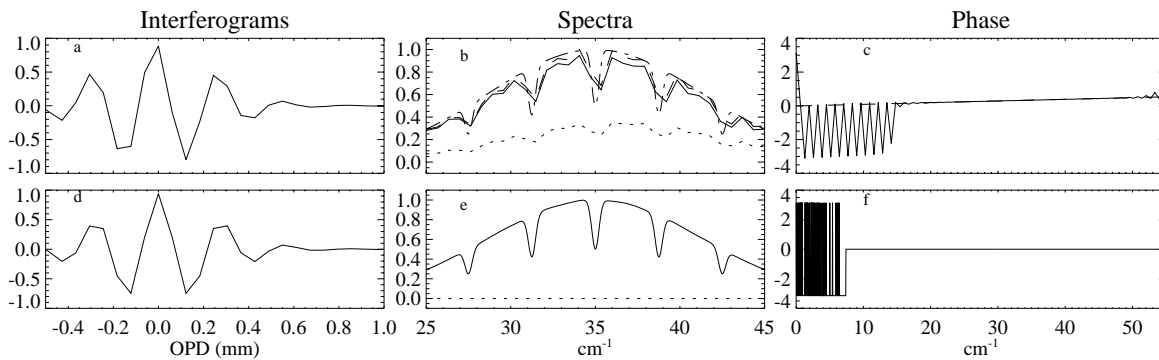


Fig. 1. Phase correction in various stages. (a) uncorrected interferogram (with phase/symmetry error), (b) uncorrected spectrum with real (solid line), imaginary (dot), abs (dash), and ideal (dash dot) case shown, (c) uncorrected phase with phase fit (dash) (d) corrected interferogram, (e) corrected spectrum with real (solid) and imaginary (dot) components shown, and (f) resultant corrected phase

3.4. Analysis

A multivariate error minimization was performed using the Gaussian line centre, width, amplitude and area as parameters. A graphical user interface (GUI) was written to allow the user to plot the error surface as a function of the various input parameters. Fig. 3 shows the control panel of the GUI and an example error surface with varied PCF (left to right) and line (front to back) widths.

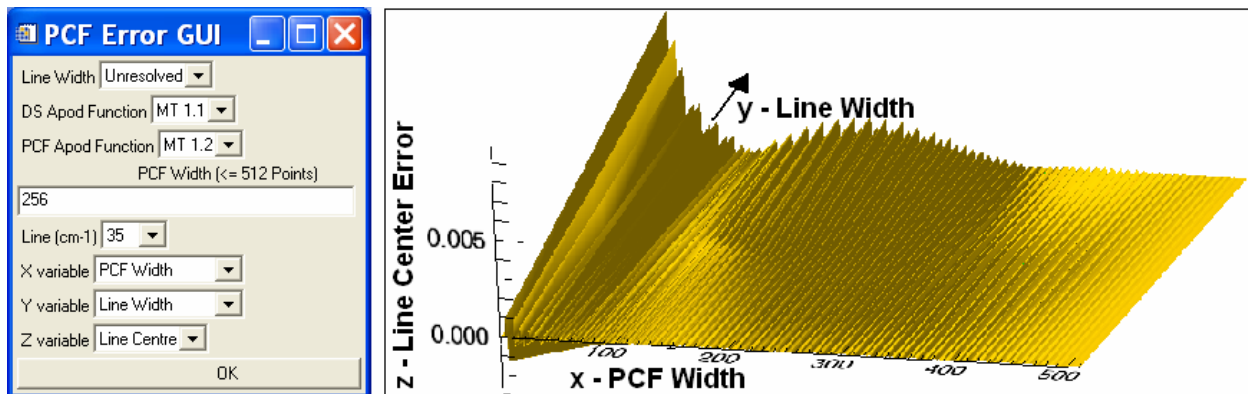


Fig. 3. Control panel for error surface generating tool (left), and sample error surface generated using parameters shown in control panel (right).

4. Conclusions and Future Work

Analysis is on-going and results will be presented at the OSA FTS/HISE 2004 meeting. Future work includes a more detailed analysis of the phase correction and apodization parameter space, and the introduction of various types of noise into the test spectra. This program is proving to be useful as a tool to study the optimum parameters for phase correction in two imaging FTS projects in which our group is involved (SPIRE and SCUBA-2) [6, 7].

5. References

1. R.J. Bell, *Introductory Fourier Transform Spectroscopy* (Academic Press, New York, 1972)
2. Forman, M.L., Steel, W.H. and Vanasee, G.A., *Correction of asymmetric interferograms obtained in Fourier transform spectroscopy*, J.O.S.A., **56**, 59 (1966)
3. B.P. Lathi, *Signal Processing and Linear Systems* (Berkeley-Cambridge Press, Carmichael, 1998), Chap. 4.
4. *Interactive Data Language*, (Research Systems Inc., Colorado, 2004), <http://www.rsinc.com>.
5. P.R. Griffiths, and J.A. Haseth, *Fourier Transform Infrared Spectrometry* (John Wiley and Sons, New York, 1986)
6. S.P. Davis, M.C. Abrams, and J.W. Brault, *Fourier Transform Spectrometry* (Academic Press, New York, 2001)
7. L.D. Spencer, D.A. Naylor, B.M. Swinyard, *et al.*, "A Fourier transform spectrometer for ground testing of the Herschel/SPIRE instrument," in *Astronomical Telescopes and Instrumentation*, Proc. SPIE, 5487, in press (2004).
8. B.G. Gom, D.A. Naylor, "An update on the imaging Fourier transform spectrometer for SCUBA-2," in *Astronomical Telescopes and Instrumentation*, Proc. SPIE, 5498, in press (2004).